

Article

Pressure Fluctuation near the Limiting Characteristics in a Sonic Flow around NACA0012 Airfoil

Lei Zhang [†] and Zi-Niu Wu ^{*,†}

Department of Engineering Mechanics, Tsinghua University, Beijing 100084, China

* Correspondence: ziniuwu@tsinghua.edu.cn

† These authors contributed equally to this work.

Abstract: Pressure fluctuation for flow around an airfoil has been well studied for subsonic, transonic and supersonic flows. In this paper, the sonic flow case is studied using a NACA0012 airfoil. It is known that such a flow has a limiting characteristic line which is known to separate the supersonic region into an upstream zone (U-zone) and a downstream zone (D-zone) where the pressure waves propagate into different directions, thus it is interesting to investigate whether the pressure fluctuation also exhibits special behavior along the limiting characteristic line. From an analysis of the pressure fluctuation properties by detached eddy simulation and method of characteristics, it is found that the pressure fluctuation exhibits different behavior in these two zones, and displays interesting properties along the limiting characteristic line. The fluctuation pressure is the largest along the limiting characteristic line, while the correlation coefficient between two adjacent points is the smallest along the limiting characteristic line. Away from the limiting characteristic line, the fluctuation pressure decays. Moreover, there is a spatial variation of the pressure fluctuation across the boundary layer. This spatial variation is in the mid-frequency band in the U-zone, in the high-frequency band in the D-zone, and in the entire-frequency band along the limiting characteristics line. The special behavior of the pressure fluctuation along the limiting characteristic line revealed by this study enriches our knowledge about transonic flow.

Keywords: fluctuating pressure; limiting characteristics; sonic flow; airfoil



Citation: Zhang, L.; Wu, Z.-N. Pressure Fluctuation near the Limiting Characteristics in a Sonic Flow around NACA0012 Airfoil. *Fluids* **2022**, *7*, 307. <https://doi.org/10.3390/fluids7090307>

Academic Editors: Mahmoud Mamou and Mehrdad Massoudi

Received: 22 July 2022

Accepted: 8 September 2022

Published: 16 September 2022

Publisher's Note: MDPI stays neutral with regard to jurisdictional claims in published maps and institutional affiliations.



Copyright: © 2022 by the authors. Licensee MDPI, Basel, Switzerland. This article is an open access article distributed under the terms and conditions of the Creative Commons Attribution (CC BY) license (<https://creativecommons.org/licenses/by/4.0/>).

1. Introduction

The pressure fluctuation of the flow near the surface of aircraft may induce damage-causing structural vibration and bothering noise environment that affects the normal operation of airborne instruments [1]. For this reason the problem of pressure fluctuation for an airfoil has received considerable interests.

For subsonic flow, the wall fluctuating pressure generated around a NACA0012 airfoil with the attack angle of 10° has been studied numerically by Wang and Tian [2], the frequency property shows that the fluctuating pressure is dominated by the vortex shedding for stationary situation and the flapping for the pitching situation, respectively. For the stationary and low frequency pitching airfoil, the fluctuation of the high frequency band induced by the vortex scattering are crucial, which is decreased by the high frequency pitching. In addition, Awasthi et al. [3] used the large eddy simulation (LES) method to simulate the characterization of the wall fluctuating pressure, the computations of pressure fluctuation around the airfoil and near the trailing-edge are consistent with the measurements in the low-to-mid frequency band, and the histogram distribution of surface pressure fluctuation within the separation bubble upstream of the airfoil shows serious streamwise difference reflecting the instantaneous nature of the flow in this region.

For transonic flow, Hillenherms and Limberg [4] has experimentally measured the fluctuating pressure on a pitching airfoil. They found that, on the upper side of the pitching airfoil, maximum fluctuation levels occur for Mach numbers of 0.72 to 0.77 which is not only

in the region of the shock but overall on the upper side, since this is likely due to a higher fluctuation level of the incoming flow. Hasan and Alam [5] used numerical simulation to investigate the fluctuating pressure over a supercritical airfoil for a fixed free-stream Mach number of 0.77 and at angle of attack varying from 2° to 7° . They found that the values of peak pressure fluctuation is increased with an increase of angle of attack, and the location of peak pressure fluctuation is shifted toward the leading edge of the airfoil with increasing angle of attack. Chen, Xu and Lu [6] used detached-eddy simulation (DES) to study pressure fluctuation at Mach number 0.76, and discovered that the velocity of downstream-propagating waves in the separated boundary layer is close to the convection speed of the coherent vortical structures, the power spectral density function (PSD) properties show that there are various spectral scalings with the frequency in different flow regions.

For supersonic flow, Messiter [7] combined the method of multiple scales and matched asymptotic expansions to derive the disturbances caused by an oscillating airfoil. They found that the oscillatory part of the pressure at a leading-edge shock wave diminishes fleetly with increasing distance from the edge. Later, fluctuating pressure around airfoil has been studied experimentally by Fleeter [8] for six different oscillating airfoil surfaces in a supersonic flowfield, and the unsteady pressure fluctuation properties is correlated with Mach number.

Past studies of airfoil pressure fluctuation have focused on the wall surface. In generally, pressure fluctuation propagates at the speed of sound, so it is imaginable that the pressure fluctuation does not vary significantly across the boundary layer. However, at least for academic purpose, it is interesting to investigate whether the variation of pressure fluctuation is indeed negligible across the boundary layer.

For a pure turbulent boundary layer, Panton, Lee and Moser [9] used direct numerical simulation (DNS) method to investigate the correlation of spatial fluctuating properties in turbulent layers, and the root-mean-square (RMS) pressure fluctuations in the inner and outer layers are correlated for different Reynolds numbers. They discovered that there are small variations of fluctuating pressure across the boundary layer and the outer layer profiles of the fluctuation properties correlate very well for various Reynolds numbers, however, the correlation in inner profiles is not excellent, and the overlap matching area has logarithmic behavior.

Zhang and Wu [10] studied the fluctuating pressure near the expansion corner in supersonic flow and found that near the corner the fluctuation pressure varies across the boundary layer. Moreover, there exists a region bounded by the characteristics lines that the variation of the pressure fluctuation is pronounced. They identified three zones: U-zone, M-zone and D-zone inside which the variation of the pressure fluctuation exhibits various behaviors, due to that disturbance in supersonic flow propagate along inside the Mach cone.

In this paper, we consider the spatial pressure fluctuation properties inside the supersonic flow region of a NACA0012 airfoil at sonic inflow condition, that is, the upstream flow Mach number is one. The reason to consider this case is that there is a limiting characteristics line in the supersonic zone, upstream and downstream of which the pressure waves propagate in different directions. It is expected that the spatial variation of pressure perturbation may exhibit similar interesting phenomena like in the supersonic expansion corner case, and more undesired properties due to the existence of limiting characteristics line.

Here, in this work, we relate the spatial distribution of the fluctuating pressure to the propagation of the characteristics around NACA0012 airfoil, at sonic inflow. In Section 2, we will introduce the sonic flow problem and numerical problem. The division of the flow domain into U-zone and D-zone according to the limiting characteristic line will be described in Section 3. The results of the spatial distribution of fluctuation properties in the two different zones are given in Section 4, where the pressure distributions properties will be measured by the root-mean-square fluctuating pressure coefficient ($C_{p_{rms}}$) and power spectral density function (PSD) [11]. The special behaviors of spatial distribution of $C_{p_{rms}}$

and PSD in U-zone and D-zone will be presented in Section 5. Finally, conclusion will be given in Section 6.

2. The Sonic Flow Problem and Numerical Method for Simulation

2.1. Sonic Flow and Limiting Characteristic Line

In the present paper we consider a two-dimensional flow around the NACA0012 airfoil at sonic inflow, i.e., the free-stream Mach number $M_\infty = 1$. At this condition, it is well-known that there is a large bulk of supersonic flow region near the airfoil and there is a limiting characteristic line [12], see Figure 1 for a schematic display of the flow.

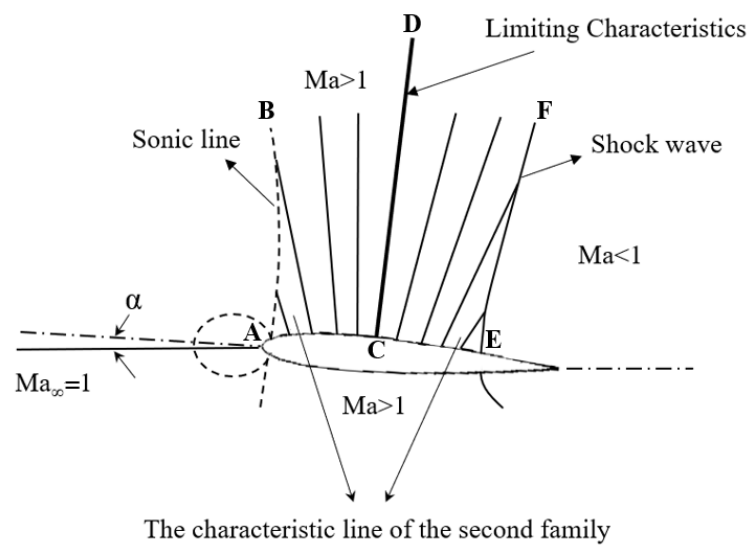


Figure 1. Limiting characteristics at the speed of sound [12].

In Figure 1, dashed lines such as AB denote sonic line and EF is the recompression shock. The limiting characteristic line, which contains the segment CD , lies between AB and EF and extends to infinity. Upstream of CD , the characteristics propagate upstream and the characteristics lines join the sonic line AB . Downstream of CD , the characteristics propagate downstream and join the recompression shock EF . The limiting characteristic line meets the sonic line AB and the recompression shock EF at infinity.

Landau and Lifshitz [12] provided the analytical formula for the shape of this limiting characteristics line, as well as the sonic line and shock wave. The coordinates of these lines are given by

$$\frac{x}{y^{\frac{4}{5}}} = \frac{k^{\frac{1}{5}}(2s - 1)}{2s^{\frac{2}{5}}} \tag{1}$$

The parameter k is an arbitrary positive constant which depends on the actual shape of the airfoil. In our case of NACA0012 airfoil, we find $k = 100$. In Equation (1), the value of s is determined by

$$s = \frac{f^2}{f^2 - \eta} \tag{2}$$

where f and η satisfy

$$f^3 - 3\eta f + 3\theta = 0, \eta = (2\alpha_*)^{\frac{1}{5}} \frac{V - c_*}{c_*} \tag{3}$$

In (3), $\alpha_* = \frac{1}{2}(\gamma + 1)$, γ is the ratio of specific heat, V is the fluid velocity, c_* is the critical speed, θ is the angle between the velocity and x -axis. When θ is small enough, the velocity $V \approx V_x$ and $c_* \approx c$, where c is the speed of sound.

The sonic line corresponds to $s = 1$, and limiting characteristic line to $s = \frac{4}{3}$, the shock line to $s = 2.78$.

2.2. Numerical Simulation Method

Various authors have used numerical simulation to study pressure fluctuation, with special attention on the choice of turbulence models, including Reynolds averaged Navier–Stokes (RANS) method (e.g., Lozano and Paniagua [13], Soni et al. [14]), detached eddy simulation (DES) method (e.g., Chen, Xu and Lu [6]), large eddy simulation (LES) method (e.g., Awasthi et al. [3]) and direct numerical simulation (DNS) method (e.g., Richard [15]).

To study the spatial distribution of fluctuation properties around an expansion corner, the present authors used DES for numerical simulation [10]. This method has been proposed by Spalart [16]. As in the previous work, the unsteady compressible Navier–Stokes equations are solved by means of the second-order-accurate implicit Roe scheme based on finite difference simulation. For unsteady computation, the time step is fixed to be $\Delta t = 1 \times 10^{-6}$ s, and the total number of time iterations is 2×10^4 . The implicit scheme involves internal iteration for each physical time step, and we require the inner-residuals of each iteration be 1×10^{-8} . We have tested three grids of different density: 50, 80 and 100 thousands of grid points, with refinement near the wall and we found that a grid of 80 thousand elements with refinement near the wall and limiting characteristics is suitable to give the required results. The mesh has a wall normal resolution of $y^+ \sim 0.5$ in the densified region (e.g., [17]), and increases smoothly at a rate 1.05 away from the wall.

We have not found experimental result of NACA0012 at sonic inflow, so we choose an inflow Mach number that is close to unity and for which we can find experimental results.

The fluctuating pressure around NACA0012 airfoil has been studied experimentally by Ren [18] with the free-stream mach number $Ma_\infty \approx 0.9$. This experiment was carried out to investigate the fluctuating wall-pressure field along chord and spanwise, and the results of the measurements of pressure coefficient (C_p) and sound pressure level (SPL) were given in this paper.

As usual, $C_{p_{rms}}$ is defined by $C_{p_{rms}} = \frac{\sqrt{\overline{p^2}}}{0.5\rho_\infty U_\infty^2}$, where ρ_∞ and U_∞ are density and velocity of the free-stream, T is the entire sampling time, p_{avg} is the average pressure during the total sampling process, $\sqrt{\overline{p^2}} = \sqrt{\frac{1}{T} \int_0^T (p(t) - p_{avg})^2 dt}$ is the rms of the fluctuating pressure, $p(t)$ is the the momentary pressure at a specified point in the flow field that is recorded during numerical simulation. PSD (denoted $\phi(\omega)$) is obtained by the Fourier transform of the pressure change in the time domain by $\phi(\omega) = \frac{1}{T} \int_0^T p(t)e^{i\omega t} dt$, where ω is the frequency (Hz).

We tested the above numerical method against the experimental results of Ren [18] and the comparison of pressure coefficient (C_p) and the sound pressure level are shown in Figure 2. It is seen that the comparison is reasonably good.

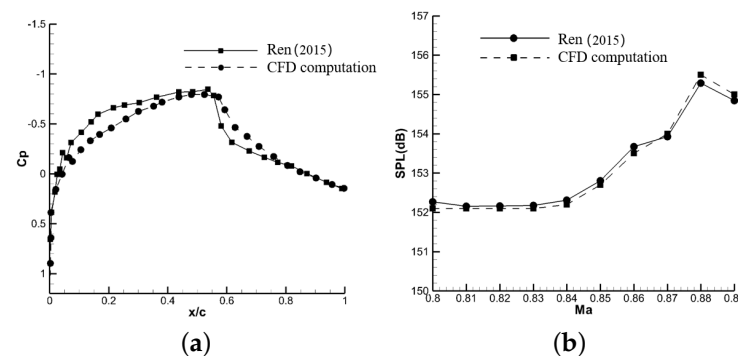


Figure 2. Comparison of results [18]. (a) Pressure Coefficient along the flow direction on the wall (c is the chord). (b) Sound Pressure Levels(SPL)at different Mach numbers ($x/c = 0.75$).

3. Limiting Characteristics and Definition of U-Zone and D-Zone

3.1. Method to Find Characteristic Lines from CFD Data

In order to define the U-zone and D-zone divided by the limiting characteristic line and distribute sampling points along the characteristic lines, we need to obtain the characteristic lines from the numerical solution of the flow field. A simple method has been described by Zhang and Wu [10]. Here we simply recall how it is used.

For the isentropic supersonic flow region, the characteristic lines are given by

$$\frac{dy}{dx} = \frac{1}{\lambda} \tag{4}$$

where λ is the eigenvalue. The value $\lambda = \lambda_1$ corresponds to the first family of characteristics, and the second family of the characteristics corresponds to $\lambda = \lambda_2$, where λ_1 and λ_2 are defined by

$$\begin{cases} \lambda_1 = \frac{uv - c^2\sqrt{Ma^2 - 1}}{v^2 - a^2} \\ \lambda_2 = \frac{uv + c^2\sqrt{Ma^2 - 1}}{v^2 - a^2} \end{cases} \tag{5}$$

and u and v are the velocity components; Ma is the Mach number; a is the speed of sound. In the present paper only the second family of characteristics is used.

Once the numerical solution of the mean flow field is obtained by numerical simulation, the expressions (4) and (5) are used to obtain the characteristic lines.

For numerical simulation of the present problem, we used a computational domain and boundary conditions as shown in Figure 3. The upstream flow is a sonic flow, with a freestream Mach number $Ma_\infty = 1$. The right boundary is a pressure exit, and the other sides are pressure far field condition. The wall has a no-slip condition. The Reynolds number based on the chord ($c = 200$ mm) is $Re_c = 4.2E + 06$, with a freestream turbulent intensity $Tu = 5\%$.

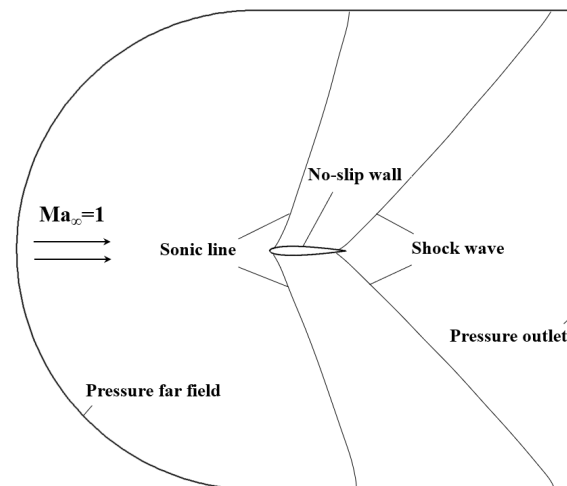


Figure 3. NACA0012 airfoil computed model.

Now we use the local flow parameters from numerical results and apply (4) and (5) to obtain the characteristic lines. The results are given in Figure 4, where we also display the sonic line, limiting characteristic line and the recompression shock wave, obtained by both theory (see (1)) and numerical simulation. As in Figure 1, AB is sonic line, CD is limiting characteristics, EF is shock wave. Note that inside the boundary layer and very close to the wall, $Ma < 1$ so that we have no real values of λ_1 and λ_2 . As in our previous work, in such regions, we simply extend the characteristic lines to the wall using straight lines.

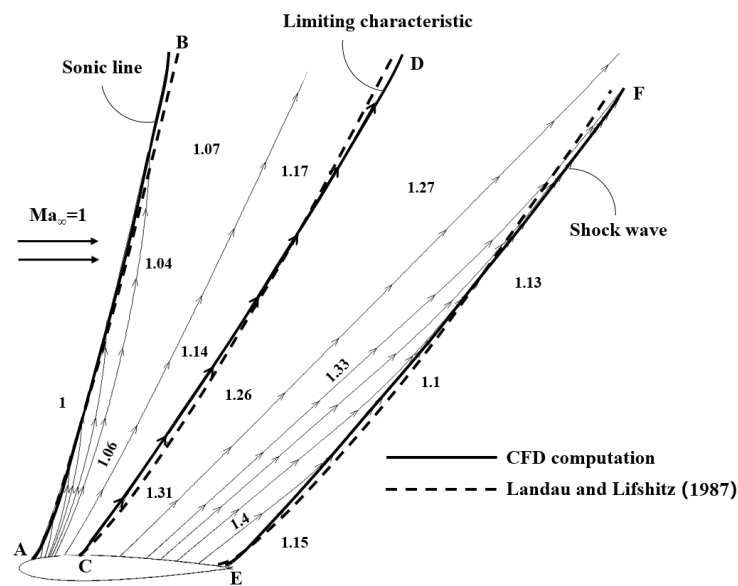


Figure 4. Limiting Characteristics in the Mach number contour map [12].

From Figure 4, we see that the theory matches the numerical simulation and that the propagation of characteristics indeed follows two different directions according to whether they are upstream and downstream of the limiting characteristic line.

3.2. Division of the U-Zone and D-Zone

For the problem of the pressure fluctuation of expansion corner, Zhang and Wu [10] have found that the region near the corner can be divided into three zones with different pressure fluctuation properties. For the present problem, since pressure disturbance propagates along the characteristic lines and since the characteristics (of second family) propagate at different direction according to whether they are upstream and downstream of the limiting characteristic line, we intend to divide the flow region into two zones: U-zone and D-zone, as shown in Figure 5. The U-zone is the region which lies between the sonic line AB and the limiting characteristics CD. The D-zone is the region which lies between the limiting characteristics CD and the shock wave EF.

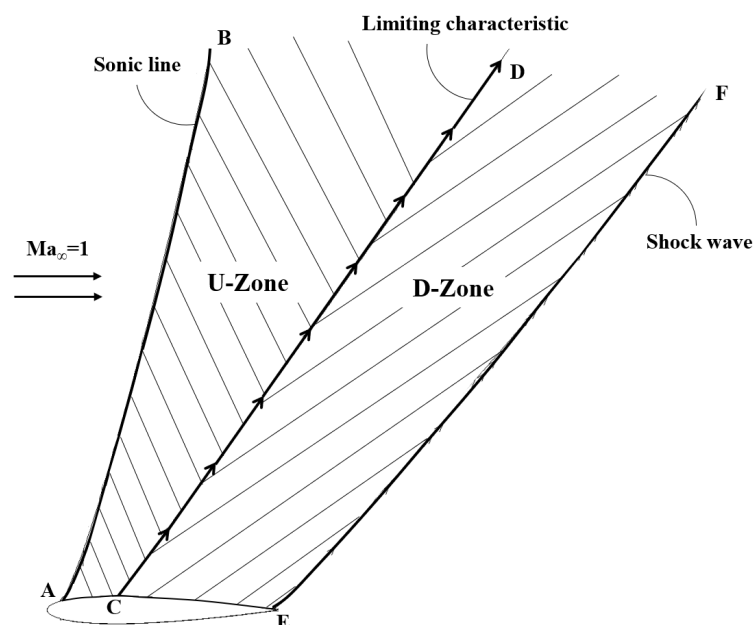


Figure 5. The U-Zone and D-Zone.

It is expected that the pressure fluctuation in the U-zone does not affect that in the D-zone, and that in the D-zone does not affect that in the U-zone.

4. The Cp_{rms} and PSD in the Various Zones

The spatial distributions of the numerical results of fluctuating pressure properties Cp_{rms} and PSD within the boundary layer are given along the direction of characteristic lines in various zones. First we discuss how the sampling points are chosen in order to study the spatial distribution related to characteristics.

4.1. Distribution of Sampling Points

The sampling points are evenly arranged at different zones along the characteristic lines around the NACA0012 airfoil, and the positions of these points are given in Figure 6. The sampling points are distributed over a finite number of characteristic lines labeled “a”, “b”, ... “g”. The limiting characteristic line CD corresponds to “d”. Thus, the characteristic lines “a”, “b”, “c” are upstream of the limiting characteristics, and the lines “e”, “f”, “g” are downstream of the limiting characteristics. Along each characteristic line, we put a point at $y^+ = 0$ (wall surface), a point at $y^+ = 30$ (inside the buffer layer), a point at $y^+ = 300$ (inside the log-law layer) and a point at $y^+ > 1000$ (inside the outer layer), and these points are labelled with subscripts “1”, “2”, “3” and “4”, respectively. The points a_i, b_i, c_i with $i = 1, 2, 3, 4$ lie in the U-zone, and the points e_i, f_i, g_i with $i = 1, 2, 3, 4$ lie in the D-zone.

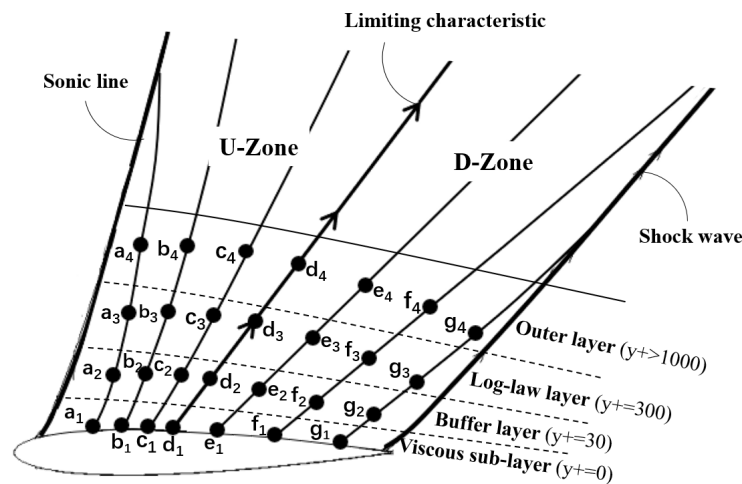


Figure 6. The distribution of measuring points.

As stated in Introduction, for airfoils the fluctuation properties have been considered mainly along the wall, possibly for reason that these properties do not vary across the boundary layer due to the rapid propagation of sound waves compared to the thickness of the boundary layer. Now we output these pressure perturbation properties at the various points as shown in Figure 6 to see if noticeable variation across the boundary layer exists and if yes how this variation is associated with the characteristic lines upstream and downstream of the limiting characteristic line.

4.2. The Distribution of Cp_{rms} in the Various Zones

The distribution of Cp_{rms} within the boundary layer obtained by numerical simulation is shown in Figure 7. The abscissa “a~g” correspond to the different characteristic lines displayed in Figure 6. The four curves correspond to the four points (1,2,3,4) inside the boundary layer as shown in Figure 6.

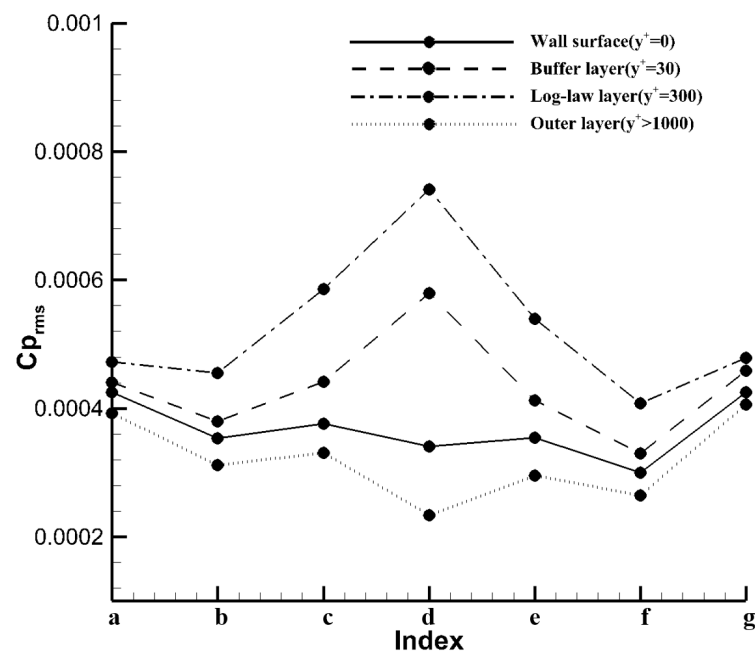


Figure 7. The distribution of Cp_{rms} within boundary layer near limiting characteristics.

As can be seen from Figure 7, Cp_{rms} varies much across the boundary layer near the limiting characteristic line, and this variation diminishes away from the limiting characteristic line. There may be some intrinsic reason for this that may need to be considered further. Moreover, Cp_{rms} has different values within the boundary layer: Cp_{rms} reaches maximum in the log-law layer ($y^+ = 300$, labeled “3”) and the minimum value in the outer layer ($y^+ > 1000$, labeled “4”). Thus, the wall pressure fluctuation is less intense than that in the log-law layer.

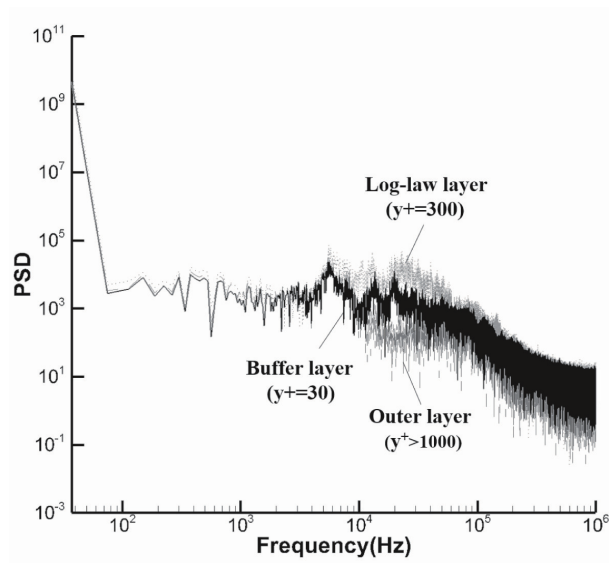
Along the characteristic line, $Cp_{rms} = 0.00074$ in the log-law layer, which is 70% larger than outer layer ($Cp_{rms} = 0.00023$) and 57% larger than wall surface ($Cp_{rms} = 0.00034$).

At point a, $Cp_{rms} = 0.00046$ in the log-law layer, which is 15% larger than outer layer ($Cp_{rms} = 0.00039$) and 8% larger than wall surface ($Cp_{rms} = 0.00042$).

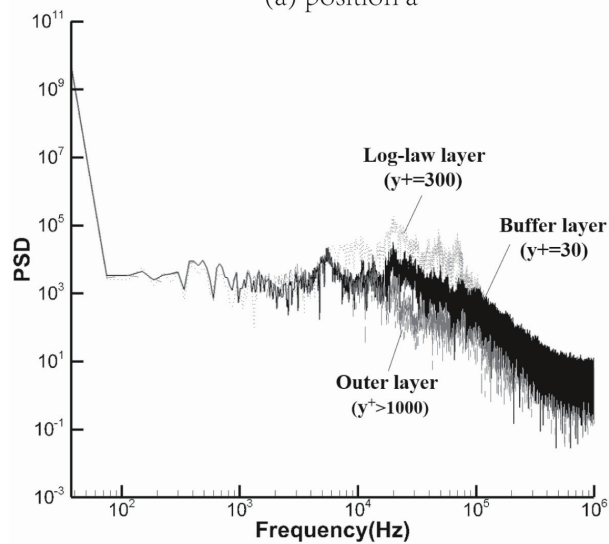
At point g, $Cp_{rms} = 0.00048$ in the log-law layer, which is 16% larger than outer layer ($Cp_{rms} = 0.00040$) and 12% larger than wall surface ($Cp_{rms} = 0.00042$).

4.3. The PSD in the Various Zones

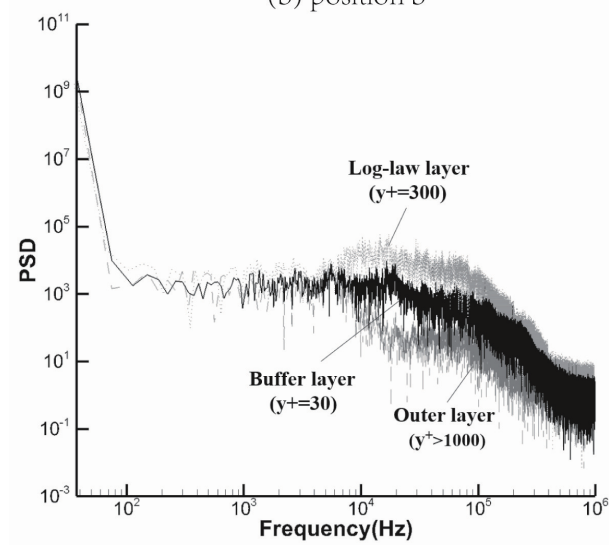
For the positions a,b,c which are upstream of the limiting characteristic line, the numerical results of PSD at locations 2, 3 and 4 in the boundary layer are displayed in Figure 8a–c. Recall that location 2 is at $y^+ = 30$ (buffer layer), location 3 is at $y^+ = 300$ (log-law layer) and location 4 is at $y^+ > 1000$ (outer layer). We see that the PSDs at the three locations have differences in the mid-frequency band, and have little difference in the low-frequency and high-frequency band. The values of PSD in the mid-frequency band first increase and then decrease with the distance from the wall. Thus, the pressure perturbation variation across the boundary layer is due to the middle-frequency perturbation. Approaching the limiting characteristics line along the flow direction, the spatial difference of PSD gradually increases. Thus, the frequency properties of fluctuating pressure show differences in the mid-frequency in “U-zone”.



(a) position a



(b) position b



(c) position c

Figure 8. PSD at positions “a~c”.

On the limiting characteristic line CD (point “d”), PSD at the locations 2, 3 and 4 are displayed in Figure 9. On the limiting characteristic line, $PSDs$ at different layers show differences over the entire-frequency band. As for points a,b,c, the values of PSD first increases and then diminishes with the distance from the wall and it reaches the maximum value at $y^+ = 300$ (log-law layer). That is, the frequency properties of fluctuating pressure show differences in the entire-frequency along the “limiting characteristics”.

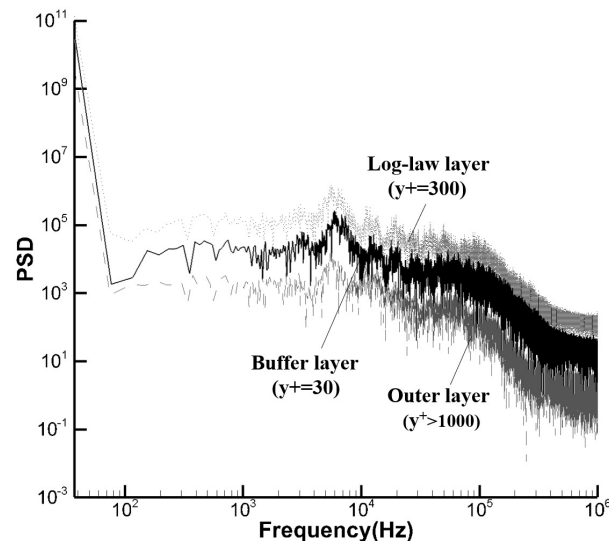
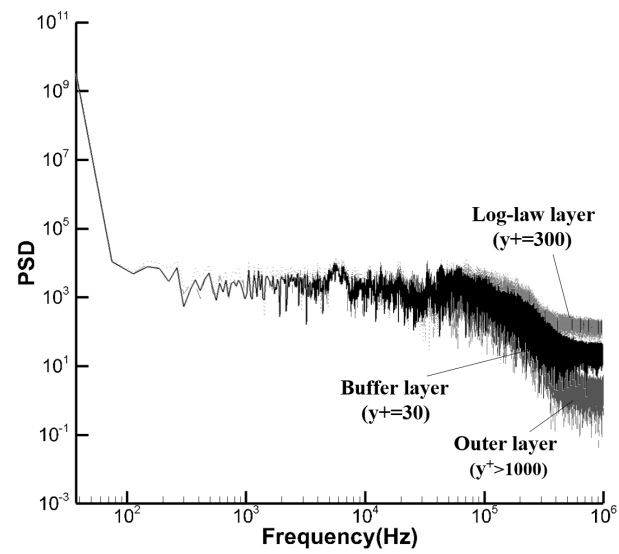
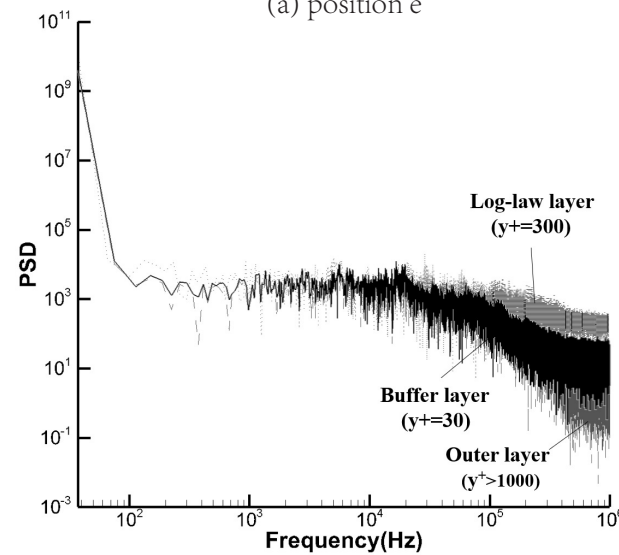


Figure 9. PSD at positions “d”.

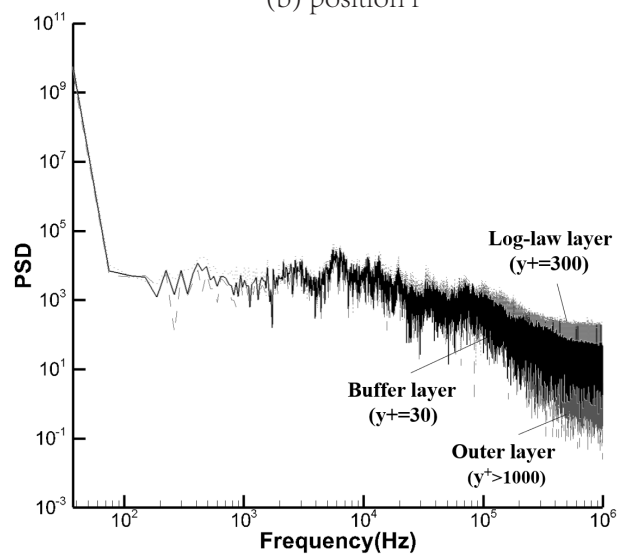
The numerical results of PSD at positions “e~g” (downstream from the limiting characteristics CD) are displayed in Figure 10. The curves of the PSD at $y^+ = 30$ (buffer layer), $y^+ = 300$ (log-law layer) and $y^+ > 1000$ (outer layer) show differences in the high-frequency band, however, they almost overlap in the low-frequency and mid-frequency band. In the flow direction away from the limiting characteristics, the difference of PSD gradually decreases. The values of PSD in the high-frequency band first increase and then decrease with the distance from the wall. That is, the frequency properties of fluctuating pressure show differences in the high-frequency in “D-zone”.



(a) position e



(b) position f



(c) position g

Figure 10. PSD at positions “e~g”.

5. Summary of Fluctuating Pressure Properties

Based on the fluctuation properties displayed in Section 4, we use Figure 11 to summarize the special behaviors of the fluctuating pressure near the limiting characteristics in a sonic flow around NACA0012 airfoil. There are two zones, U-zone and D-zone, as introduced in Section 3.

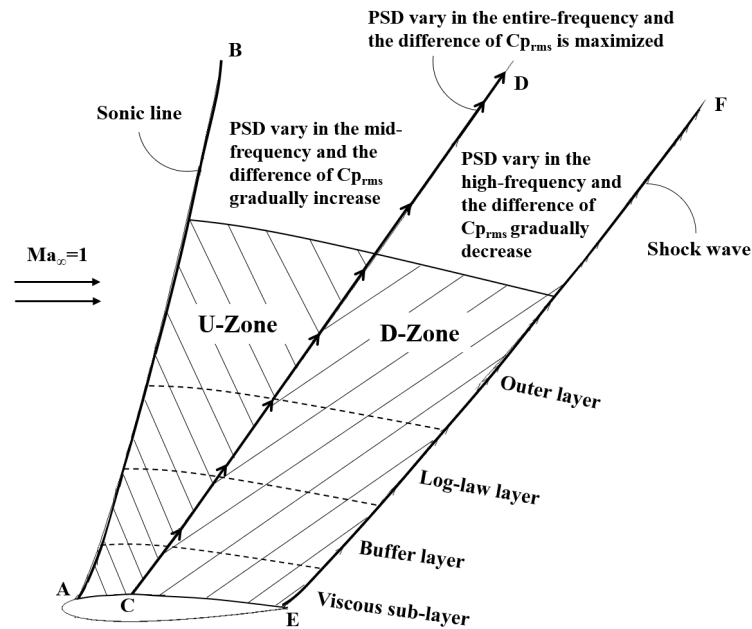


Figure 11. The pressure fluctuation in the U-zone and D-zone.

In the U-zone which is upstream of the limiting characteristics, there is spatial variation of Cp_{rms} across the boundary and this variation becomes important when approaching the limiting characteristics. In the D-zone which is downstream of the limiting characteristics, the spatial variation of Cp_{rms} gradually increases when approaching the limiting characteristic line. The spatial variation of Cp_{rms} is the largest along the limiting characteristic line, showing an interesting property of the limiting characteristic line.

Upstream of the limiting characteristic line, PSD shows spatial variation mainly in the middle-frequency band, downstream of the limiting characteristic line the spatial variation of PSA occurs mainly in the high-frequency band, and along the limiting characteristic line this variation occurs over the entire-frequency band.

It is funny to see the correlation of unsteady pressure at two different layers near the limiting characteristic line. The correlation coefficient (named r_{AB}) of the transient pressure data at two positions A and B is defined by

$$r_{AB} = \frac{cov(p_A(t), p_B(t))}{\sqrt{Var[p_A(t)] \cdot Var[p_B(t)]}} \tag{6}$$

where $p_x(t)$ is the transient pressure at a certain point x ; $cov(p_A(t), p_B(t))$ is the covariance of $p_A(t)$ and $p_B(t)$; $Var[p_x(t)]$ is the variance of $p_x(t)$.

The distribution of r_{AB} near the limiting characteristics calculated by Equation (6) is shown in Figure 12, where we displayed r_{AB} between the wall surface and the buffer layer, r_{AB} between the buffer layer and log layer, and r_{AB} between the log layer and the outer layer. It is strange that the correlation between different points is the minimal along the limiting characteristic line. Thus, not only the limiting characteristic line has no interaction with the adjacent characteristic lines, the interaction between various locations along this limiting characteristic line is also the smallest.

We observe that a phenomenon occurs both in the U-zone and D-zone. If point A and point B are far from the limiting characteristics (such as position “a” and “g”), the

correlation coefficient is a little bit less than 1. If point A and point B are along the limiting characteristics (position “d”), the correlation coefficient is much lower than 1.

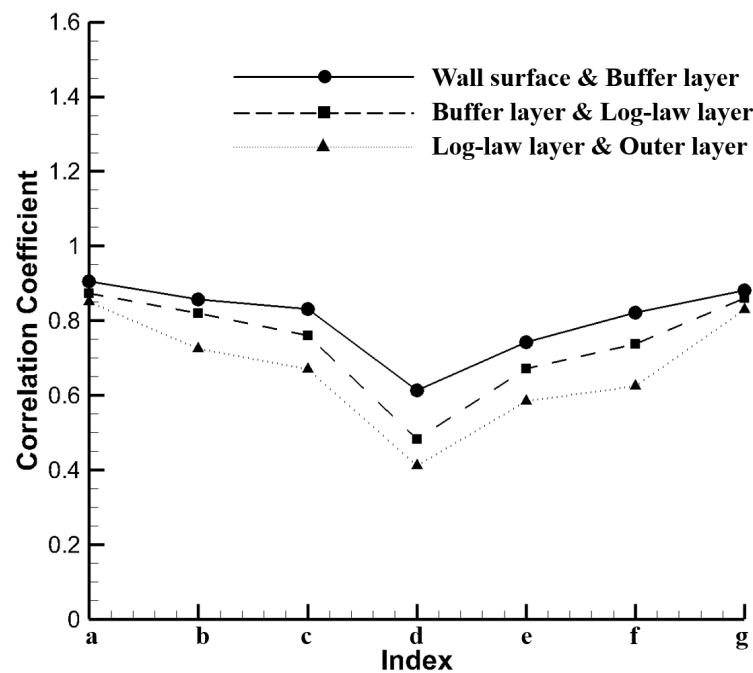


Figure 12. The distribution of the correlation coefficient between different layers near the limiting characteristics.

6. Conclusions

In this work, the pressure fluctuation properties near the limiting characteristics in a sonic flow (the mach number of inflow is $Ma_\infty = 1$) around NACA0012 airfoil is studied using numerical method based on DES. The characteristic lines are obtained using the formula for characteristics and using numerical results of flow as input data. The limiting characteristic line is used to divide the supersonic flow zone into two zones: U-zone and D-zone. U-zone is upstream of the limiting characteristic line and D-zone is downstream of this line.

We studied the pressure fluctuation properties inside the U-zone and D-zone, and along the limiting characteristic line. In the U-zone which lies between the sonic line and the limiting characteristics, the values of Cp_{rms} differ along the characteristic lines within the boundary layer, and the difference gradually increases approaching the limiting characteristics, the variation of PSD occurs in the mid-frequency band in this region, and the correlation coefficient between two adjacent layers is less than 1.

Along the limiting characteristics, both Cp_{rms} and PSD change significantly in different layers within the boundary layer and the variation of PSD occurs in the entire-frequency band. The correlation coefficient between two adjacent layers is the smallest.

In the D-zone which lies between the limiting characteristics and shock wave, in the process of leaving the limiting characteristics, the variation of Cp_{rms} gradually decreases in different layers along the characteristic lines, the difference of PSD occurs in the high-frequency band in this region, and the correlation coefficient between two adjacent layers is less than 1.

Thus, the fluctuation pressure and its spatial variation across the boundary layer is strongly determined by the limiting characteristic line. The fluctuation pressure is the largest along the limiting characteristic line, while the correlation coefficient between two adjacent points is the smallest along the limiting characteristic line. Since the waves upstream and downstream of the limiting characteristic line propagate away from the limiting characteristic line, the present finding raises an unanswered question: why the

pressure fluctuation is the largest along this line. Away from the limiting characteristic line, the fluctuation pressure decays. There is a spatial variation of the pressure fluctuation across the boundary layer and this spatial variation is in the mid-frequency band in the U-zone, in the high-frequency band in the D-zone, and in the entire-frequency band along the limiting characteristics line. This study revealed a special behavior of the pressure fluctuation along the limiting characteristic line, which not only enriches our knowledge about transonic flow but also raises the question why the pressure fluctuation is the largest along the limiting characteristic line.

Author Contributions: L.Z. and Z.-N.W. have equally contributed to the work. All authors have read and agreed to the published version of the manuscript.

Funding: This work was supported partly by the National Key Project (Grant No. GJXM92579) and the National Science and Technology Major Project 2017-II-003-0015.

Institutional Review Board Statement: Not applicable.

Informed Consent Statement: Not applicable.

Data Availability Statement: Not applicable.

Conflicts of Interest: The authors declare no conflict of interest.

References

1. Shiwei, M.; Huabing, J. Discussion on prediction methods of fluctuating pressure environments of flow fields surrounding the aircraft. *Equip. Environ. Eng.* **2021**, *18*, 014–022.
2. Wang, L.; Tian, F.B. Sound generated by the flow around an airfoil with an attached flap: From passive fluid-structure interaction to active control. *J. Fluids Struct.* **2022**, *111*, 103571. [[CrossRef](#)]
3. Awasthi, M.; Yauwenas, Y.; Rowlands, J.; Moreau, D.; Doolan, C.J. Characterization of the Fluctuating Pressure Field in the Airfoil-Wall Junction: Measurements and Computations. In Proceedings of the 2018 AIAA/CEAS Aeroacoustics Conference, Atlanta, GA, USA, 25–29 June 2018; pp. 105–177. [[CrossRef](#)]
4. Hillenherms, C.; Schröder, W.; Limberg, W. Experimental investigation of a pitching airfoil in transonic flow. *Aerosp. Sci. Technol.* **2004**, *8*, 583–590. [[CrossRef](#)]
5. Hasan, A.B.M.; Alam, M. RANS Computation of Transonic Buffet over a Supercritical Airfoil. *Procedia Eng.* **2013**, *56*, 303–309. [[CrossRef](#)]
6. Chen, L.W.; Xu, C.Y.; Lu, X.Y. Numerical investigation of the compressible flow past an aerofoil. *J. Fluid Mech.* **2010**, *643*, 97–126. [[CrossRef](#)]
7. Messiter, A.F.; Woodruff, S.L. The far field of an oscillating airfoil in supersonic flow. *J. Fluid Mech.* **1987**, *183*, 175–183. [[CrossRef](#)]
8. Fleeter, S.; Riffel, R.E. Time-variant aerodynamics of oscillating airfoil surfaces in a supersonic flowfield. *AIAA J.* **1979**, *17*, 79–106. [[CrossRef](#)]
9. Panton, R.L.; Lee, M.; Moser, R.D. Correlation of pressure fluctuations in turbulent wall layers. *PRFLUIDS* **2017**, *2*, 094604. [[CrossRef](#)]
10. Zhang, L.; Wu, Z.N. Numerical Simulation of Pressure Fluctuation Near an Expansion Corner in a Supersonic Flow of $M = 3.01$. *Fluids* **2021**, *6*, 268. [[CrossRef](#)]
11. Beresh, S.J.; Henfling, J.F.; Spillers, R.W.; Pruett, B.O.M. Fluctuating wall pressures measured beneath a supersonic turbulent boundary layer. *Phys. Fluids* **2011**, *23*, 075–110. [[CrossRef](#)]
12. Landau, L.D.; Lifshitz, E.M. *Fluid Mechanics, Course of Theoretical Physics*; Oxford Pergamon Press: Oxford, UK, 1987; Volume 6, pp. 1–539.
13. Lozano, F.; Paniagua, G. Airfoil leading edge blowing to control bow shock waves. *Sci. Rep.* **2020**, *10*, 21922. [[CrossRef](#)] [[PubMed](#)]
14. Soni, R.K.; Arya, N.; De, A. Numerical simulation of supersonic separating-reattaching flow through RANS. *J. Phys. Conf. Ser.* **2017**, *822*, 012–037. [[CrossRef](#)]
15. Sandberg, R. Compressible-Flow DNS with Application to Airfoil Noise. *Flow Turbul. Combust.* **2015**, *95*, 211–229. [[CrossRef](#)]
16. Spalart, P.R.; Jou, W.; Strelets, M.; Allmaras, S. Comments on the feasibility of LES for wings and on a hybrid RANS/LES approach. In Proceedings of the 1st AFOSR International Conference on DNS/LES, Ruston, AP, USA, 1 June 1997; pp. 181–195.
17. Guilmineau, E.; Deng, G.; Wackers, J. Numerical simulation with a DES approach for automotive flows. *J. Fluids Struct.* **2011**, *27*, 807–816. [[CrossRef](#)]
18. Xudong, R.; Zijie, Z.; Chao, G.; Feng, L. Experimental study on buffeting phenomenon of NACA0012 airfoil. *Eng. Mech.* **2015**, *32*, 236–242.